Protein Cell 2013, 4(6): 456–466
DOI 10.1007/s13238-013-3019-8

Protein & Cell

RESEARCH ARTICLE

Cytosolic Ca^{2+} as a multifunctional modulator is required for spermiogenesis in *Ascaris suum*

Yunlong Shang[1,2], Lianwan Chen[1], Zhiyu Liu[1,2], Xia Wang[1], Xuan Ma[1], Long Miao[1]✉

[1] Laboratory of Noncoding RNA, Institute of Biophysics, Chinese Academy of Sciences, Beijing 100101, China
[2] University of Chinese Academy of Sciences, Beijing 100049, China
✉ Correspondence: lmiao@moon.ibp.ac.cn
Received March 6, 2013 Accepted April 7, 2013

ABSTRACT

The dynamic polar polymers actin filaments and microtubules are usually employed to provide the structural basis for establishing cell polarity in most eukaryotic cells. Radially round and immotile spermatids from nematodes contain almost no actin or tubulin, but still have the ability to break symmetry to extend a pseudopod and initiate the acquisition of motility powered by the dynamics of cytoskeleton composed of major sperm protein (MSP) during spermiogenesis (sperm activation). However, the signal transduction mechanism of nematode sperm activation and motility acquisition remains poorly understood. Here we show that Ca^{2+} oscillations induced by the Ca^{2+} release from intracellular Ca^{2+} store through inositol (1,4,5)-trisphosphate receptor are required for *Ascaris suum* sperm activation. The chelation of cytosolic Ca^{2+} suppresses the generation of a functional pseudopod, and this suppression can be relieved by introducing exogenous Ca^{2+} into sperm cells. Ca^{2+} promotes MSP-based sperm motility by increasing mitochondrial membrane potential and thus the energy supply required for MSP cytoskeleton assembly. On the other hand, Ca^{2+} promotes MSP disassembly by activating Ca^{2+}/calmodulin-dependent serine/threonine protein phosphatase calcineurin. In addition, Ca^{2+}/camodulin activity is required for the fusion of sperm-specific membranous organelle with the plasma membrane, a regulated exocytosis required for sperm motility. Thus, Ca^{2+} plays multifunctional roles during sperm activation in *Ascaris suum*.

KEYWORDS spermiogenesis, Ca^{2+}, major sperm protein, *Ascaris suum*

INTRODUCTION

The establishment and maintenance of cell polarity is essential for many biological processes such as embryogenesis, immune surveillance and wound healing. Typically, actin and microtubule cytoskeletons are employed to establish and maintain cell polarity (Li and Gundersen, 2008). Spermiogenesis (sperm activation), in which round sessile spermatids differentiate into asymmetric motile spermatozoa, is a symmetry-breaking process. Dynamic and pronounced morphological changes occur in the radially symmetrical spermatids during the process of mammalian sperm activation, including the formation of an elongated nucleus with condensed chromatin covered by a well-shaped acrosome in the head and a long flagellum. Cytoskeletal networks composed of actin filaments, intermediate filaments and microtubules are required for this morphological transformation during spermiogenesis (Sperry, 2012). Remarkably, this acquisition of function occurs while these cells are transcriptionally and translationally silent and is therefore highly dependent on posttranslational modifications to their existing protein components. In addition, intracellular Ca^{2+} and Ca^{2+}-dependent proteolysis have also been implicated in mammalian spermiogenesis (Berrios et al., 1998; Ben-Aharon et al., 2005).

Nematode sperm also require a functional maturation process, in which round immotile spermatids transform into asymmetrical crawling spermatozoa, to achieve fertilizing competence in the female reproductive tract (Ma et al., 2012). Upon activation, sperm extend a single pseudopod for migration, instead of the beating flagellum found in mammalian spermatozoa. In nematode *Ascaris suum* (*Ascaris* hereafter), vas deferens extract (VDE) has the capacity to trigger sperm activation (Abbas and Foor, 1978). Our previous studies demonstrate that a trypsin-like serine protease As_TRY-5 purified from VDE was identified as the sperm activator (Zhao et al., 2012). Its homolog in *C. elegans* was identified as the male sperm activator by genetic approaches (Smith and Stanfield, 2011).

Nematode sperm possess neither actin nor tubulin; instead,

their activation and amoeboid migration depend on controlled assembly/disassembly of the major sperm protein (MSP) cytoskeleton (Roberts and Stewart, 2000). During sperm activation, the sperm specific membranous organelle (MO) derived from endoplasmic reticulum/Golgi apparatus fuses with the plasma membrane (PM), leaving a permanent invagination on the cell surface and resulting in the exocytosis and translocation of MOs components (Washington and Ward, 2006; Zhao et al., 2012). In flagellated sperm, Ca^{2+} modulates nearly every step of sperm maturation and fertilization including sperm capacitation, hyperactivation, chemotaxis, acrosome reaction and sperm-egg recognition (Breitbart, 2002; Kirichok et al., 2006; Kaupp et al., 2008; Teves et al., 2009). However, the role of Ca^{2+} in nematode sperm activation was seldom reported. Previously, Ca^{2+} was implicated in the regulation of *C. elegans* sperm activation (Shakes and Ward, 1989; Washington and Ward, 2006). However, the underlying mechanisms remain to be elucidated. Here we show that cytosolic Ca^{2+} oscillations regulated by phospholipase C (PLC) and inositol (1,4,5)-trisphosphate receptor (IP_3R) synchronize with sperm activation in *Ascaris*. Ca^{2+} promotes MSP-based sperm motility by increasing mitochondrial membrane potential and thus the energy production required for MSP cytoskeleton assembly, and by modulating the activity of Ca^{2+}/calmodulin-dependent serine/threonine protein phosphatase calcineurin (CaN) for inhibiting MSP assembly and promoting MSP disassembly. In addition, we show that Ca^{2+}/calmodulin activity is required for the sperm exocytosis, which is necessary for functional spermatozoa migration. Thus, Ca^{2+} plays multifunctional roles in *Ascaris* sperm activation.

RESULTS

Cytosolic Ca^{2+} oscillations synchronize with pseudopod extension during sperm activation

To elucidate the molecular mechanism underlying Ca^{2+} modulation of the MSP-based cytoskeletal dynamics during nematode sperm activation, *Ascaris* sperm were employed as they have the following advantages: (i) *Ascaris* spermatids and their endogenous activator VDE (Zhao et al., 2012) can be obtained in large quantities; (ii) sperm activation can be studied *ex vivo*; (iii) the motile apparatus of *Ascaris* sperm can be reconstituted *in vitro* (Italiano et al., 1996; Miao et al., 2003). To investigate the roles of Ca^{2+} in sperm activation, we labeled cytosolic Ca^{2+} with Fluo 4-AM, a cell-permeable indicator, and monitored intensity dynamics of Fluo 4 fluorescence during *Ascaris* sperm activation. We detected Ca^{2+} oscillations (amplitude: $\Delta F/F0 = 0.18 \pm 0.01$) during VDE-induced sperm activation (Fig. 1A and 1B) compared with the mock control: sperm treated with heat-inactivated VDE (H-VDE) (Fig. 1C and 1D). The concert between cytosolic Ca^{2+} concentration (or $[Ca^{2+}]_i$ hereafter) oscillations and sperm morphological changes from round immobile spermatids to crawling amoeboid spermatozoa implies that cytosolic Ca^{2+} oscillations might be involved in regulating sperm activation.

Both pseudopod extension and MO fusion with the PM upon activation are required for sperm motility and male fertility (L'Hernault, 2009). *C. elegans* spermatids from the MO fusion-defective mutant *fer-1* extend pseudopods in response to the artificial activator (Washington and Ward, 2006), indicating that MO fusion and pseudopod extension are two separate events during sperm activation. Pseudopod extension can be visualized under light microscopy and the fused MOs can be detected as fluorescent puncta of FM1–43 formed at the rear edge of the cell body (Washington and Ward, 2006; Zhao et al., 2012). Our *ex vivo* time-lapse imaging showed that pseudopod protrusion precedes MO fusion (Fig. 1E and Movie S1). The following analyses dissect the roles of Ca^{2+} in pseudopod extension and MO fusion.

Ca^{2+} oscillations are required for sperm activation and are regulated by IP_3R and PLC

The rise of cytoplasmic Ca^{2+} levels during sperm activation might be caused by the influx of extracellular Ca^{2+} or the release of Ca^{2+} from intracellular store. Nematode spermatids can be activated in Ca^{2+}-free medium (Movie S2) (Ward et al., 1983; Washington and Ward, 2006), indicating that the $[Ca^{2+}]_i$ increase might be caused by Ca^{2+} release from intracellular store. Ca^{2+} oscillations are primarily regulated by IP_3R (Berridge, 2007), which can be activated by inositol (1,4,5)-trisphosphate (IP_3) generated through cleavage of phosphatidylinositol 4,5-bisphosphate (PIP_2) by PLC in a variety of cell types (Berridge, 2007). To investigate whether the IP_3/Ca^{2+} signaling cascade is required for sperm pseudopod extension and MO fusion, we treated spermatids with U73122, a specific PLC inhibitor (Gulbransen et al., 2012) or with 2-APB, a cell-permeable IP_3R inhibitor (Estrada et al., 2001), and found that both U73122 (100 μmol/L) and 2-APB (200 μmol/L) blocked VDE-induced sperm activation. These drugs inhibited both pseudopod formation and MO fusion, whereas the inactive analog of U73122, U73343, had no inhibitory effect on MO fusion and much less influence on pseudopod formation (Fig. 2A). Pseudopod extension was inhibited for ~85% and ~80% of the sperm treated with U73122 and 2-APB, respectively (Fig. 2B). Consistent with the FM1-43 staining assay (Fig. 2A, bottom panels), immunoblot results also showed that U73122 and 2-APB inhibited VDE-triggered secretion of As_SRP-1 (Fig. 2C and 2D), which was previously identified as an MO component (Zhao et al., 2012).

To validate the inhibitory effect of 2-APB on IP_3R, the $[Ca^{2+}]_i$ dynamics of 2-APB-treated cells were examined. Time-lapse imaging of Ca^{2+} oscillations revealed that VDE could not induce $[Ca^{2+}]_i$ oscillations in 2-APB-pretreated sperm (Fig. 2E and 2F). These data suggest that the Ca^{2+} oscillations regulated by IP_3R and PLC are necessary for both pseudopod extension and MO fusion during sperm activation.

Chelation of cytosolic Ca^{2+} blocks pseudopod extension but not MO fusion

To further investigate the role of Ca^{2+} in sperm activation, we depleted the cytosolic Ca^{2+} with the cell-permeable Ca^{2+} chela-

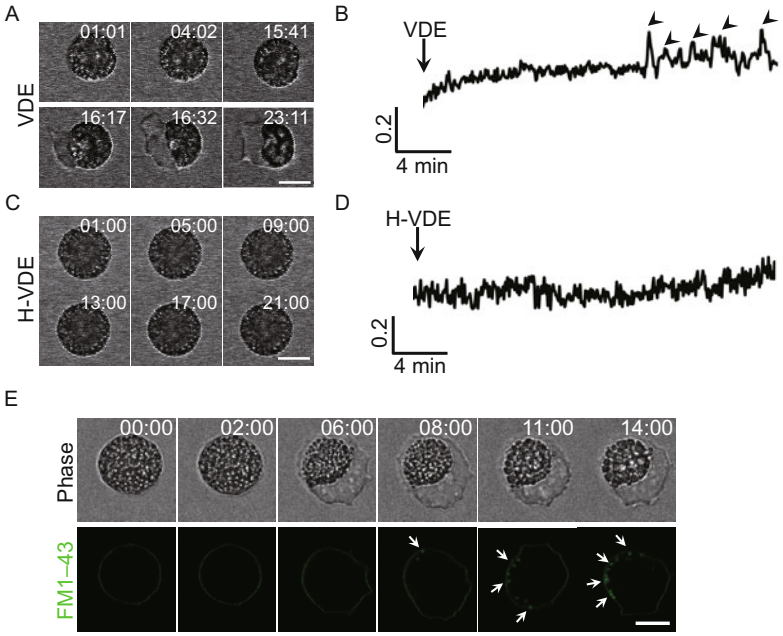

Figure 1. Sperm cytosolic Ca^{2+} oscillations were detected during *Ascaris* sperm activation. Spermatids were stimulated with vas deferens extract (VDE) (A) or heat-inactivated VDE (H-VDE) (C). The time-lapse images of sperm morphological changes were captured using a CCD camera. Scale bars, 10 μm. Traces in (B) and (D) show $[Ca^{2+}]_i$ dynamics of cells in (A) and (C), respectively, with the abscissa axis as time (min), the vertical axis as ΔF/F0. ΔF/F0 represents the relative change of fluorescence intensity against the mean baseline fluorescence intensity. The arrows indicate the time of VDE or H-VDE application. (E) Spermatids were pre-stained with FM1–43 and stimulated with VDE. Representative fluorescence and phase-contrast microscopy frames from time-lapse videos (Movie S1) show that pseudopod protrusion precedes MO fusion. Arrows mark the bright fluorescent puncta where MOs have fused with the PM.

tor BAPTA-AM (50 μmol/L). The BAPTA-AM-pretreated spermatids were stimulated with VDE and were subjected to time-lapse imaging under confocal microscope. Surprisingly, after stimulation of VDE, a small pseudopod protruded out briefly and then retracted back to the cell body (Fig. 3A and Movie S3). In contrast, in control assay the sperm pseudopod formed normally and maintained its dynamics for a much longer time (Movie S2). Consistent with the pseudopod dynamic changes, only one cytosolic Ca^{2+} transient occurred after the stimulation of VDE in BAPTA-AM-pretreated sperm (Fig. 3B). This indicated that, upon Ca^{2+} release, BAPTA-AM was unable to chelate all the released Ca^{2+}, and trace Ca^{2+} temporarily escaped from chelation. Our data further showed that BAPTA-AM blocked VDE-induced pseudopod formation significantly, in that fewer than 24% of the BAPTA-AM-treated sperm extruded a pseudopod; in contrast, 84% of the control cells showed this behavior ($P < 0.001$) (Fig. 3C and 3D). Similarly, pretreatment with another cell-permeable Ca^{2+} chelator, EGTA-AM (600 μmol/L) also prevented VDE from inducing pseudopod formation (Fig. S1).

We also examined the effect of intracellular Ca^{2+} chelation on MO fusion. The FM1-43 staining assay showed that MO fusion occurred in BAPTA-AM-treated sperm (Fig. 3C). As_SRP-1 from the cells treated with and without BAPTA-AM was secreted at similar levels (Fig. 3E), consistent with the FM1-43 staining assay. Likewise, MO fusion also occurred in EGTA-AM-treated sperm (Fig. S1). Hence, cytosolic Ca^{2+} depletion does not inhibit VDE-triggered MO fusion. The symmetrical distribution of fused MOs beneath the plasma membrane of BAPTA-AM-treated sperm (Fig. 3C, right bottom panel) indicates that sperm cell polarity is dependent on pseudopod extension but not on MO fusion.

To confirm the cytosolic Ca^{2+} depletion assay, we introduced Ca^{2+} back into the BAPTA-AM-treated sperm using the Ca^{2+} ionophore A23187 (2.5 μmol/L) and examined whether the exogenous addition of Ca^{2+} could rescue pseudopod formation. Our result revealed that Ca^{2+} ionophore combined with 100 μmol/L Ca^{2+} recovered pseudopod extension for a few minutes (Fig. 3F and Movie S4). In contrast, the cells did not respond to Ca^{2+} ionophore alone in a Ca^{2+}-free buffer (Fig. S2).

To determine whether Ca^{2+} is sufficient to induce sperm activation, we introduced different concentrations of Ca^{2+} into spermatids via Ca^{2+} ionophore A23187 treatment in the absence of VDE. This introduced Ca^{2+} failed to trigger sperm activation (Fig. S3). Collectively, these analyses demonstrate that Ca^{2+} is necessary but not sufficient to trigger sperm activation.

Ca^{2+} regulates pseudopod extension by modulating mitochondrial membrane potential

Because Ca^{2+} is an important regulator of ATP production in mitochondria (Griffiths and Rutter, 2009), and ATP is necessary for MSP assembly *in vitro* (Italiano et al., 1996), we hypothesized that Ca^{2+} regulated sperm activation by means of modulating ATP production. To test this hypothesis, we firstly examined the status of sperm activation when ATP production is defective. Our result showed that once the mitochondrial membrane potential was impaired by CCCP, which is a proton ionophore, both MO fusion and pseudopod extension were totally blocked (Fig. 4A). This fact suggests that ATP is necessary for sperm activation. Next, we investigated whether chelation of intracellular Ca^{2+} would change intracellular ATP concentration. We examined the ATP concentration in sperm with or without BAPTA-AM treatment over the course of VDE stimulation. Our result showed that in normally activated sperm, the ATP level increases dramatically after a short time of VDE stimulation, and subsequently falls down to a low level. In

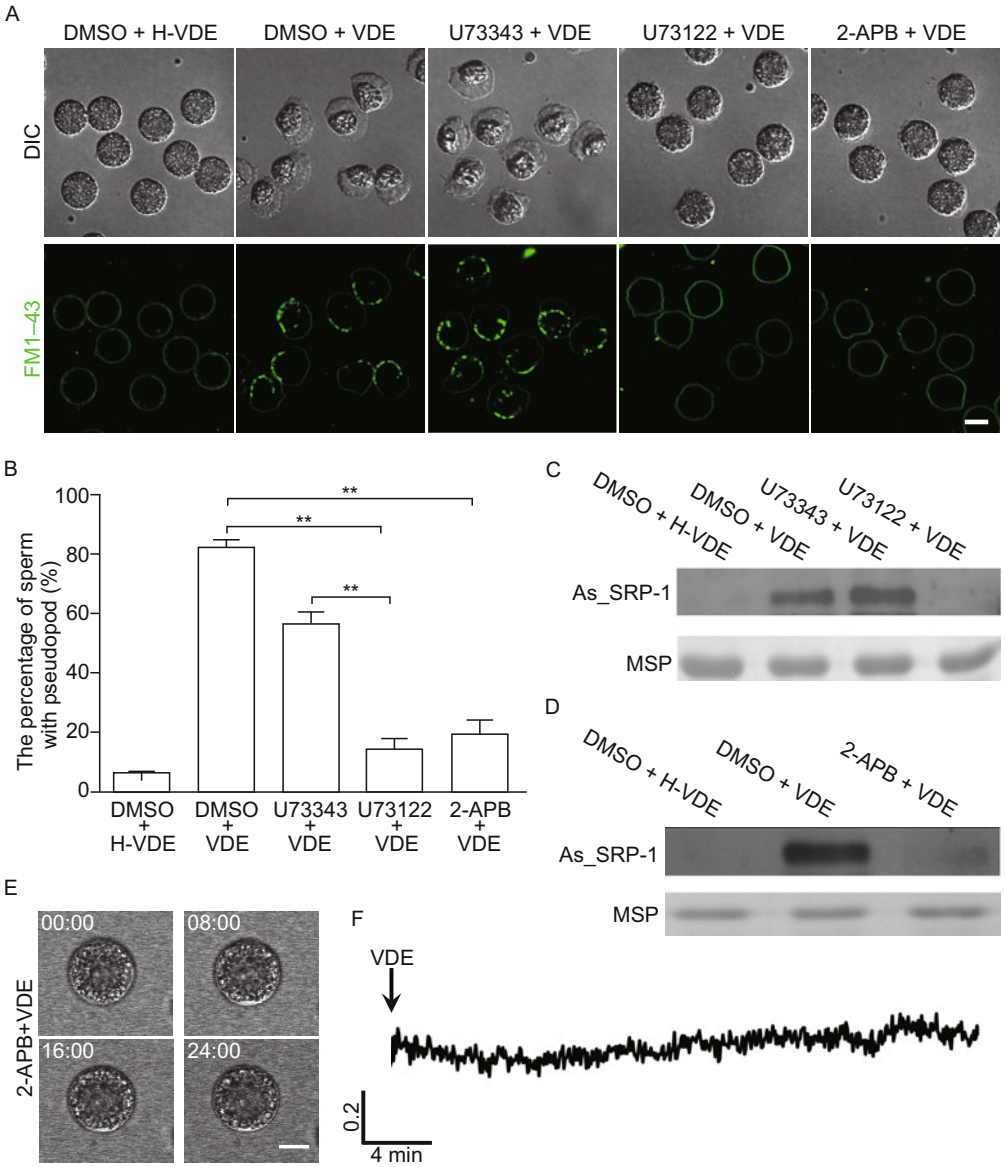

Figure 2. Ca^{2+} oscillations regulated by PLC and IP_3R are required for *Ascaris* sperm activation. (A) Both U73122 (100 μmol/L) and 2-APB (200 μmol/L) inhibits the pseudopod extension and MO fusion induced by VDE, whereas U73343 (100 μmol/L), the inactive analog of U73122, has no obvious influence on sperm activation. Spermatids were pretreated with U73122, U73343 (control for U73122) or 2-APB and then stimulated with VDE. In control, spermatids were pretreated with DMSO and then activated with VDE or H-VDE. All cells were stained with FM1–43 after the treatments. Scale bar, 10 μm. (B) Analysis of the inhibitory effects of 2-APB or U73122 on pseudopod extension. Values are the mean ± standard error of the mean (SEM) (n = 8). ** P < 0.001. (C and D) The effects of inhibitors on VDE-induced As_SRP-1 secretion. MSP was used as a loading control. (E and F) 2-APB inhibits the formation of VDE-triggered Ca^{2+} oscillations. The dynamics of sperm morphological changes (E) and Fluo-4 fluorescence (F) in sperm treated with 200 μmol/L 2-APB followed by VDE. The abscissa axis: time (min); the vertical axis, ΔF/F0. The time for VDE application is marked as "00:00". All the time stamps shown in (E) are coded in the format of min:sec. Scale bar, 10 μm.

contrast, in BAPTA-AM treated sperm, the ATP level increases weakly after VDE stimulation and then remains at a low level (Fig. 4B). This result suggests that enhanced production of ATP is required for pseudopod extension. Further, we determined the effect of BAPTA-AM on mitochondrial membrane potential which is a marker for mitochondrial activity using the fluorescent dye JC-1. The JC-1 staining assay showed that the mitochondrial membrane potential in BAPTA-AM-treated cells was significantly lower than that in controls (Fig. 4C). This fact suggests that BAPTA-AM prevents pseudopod extension by

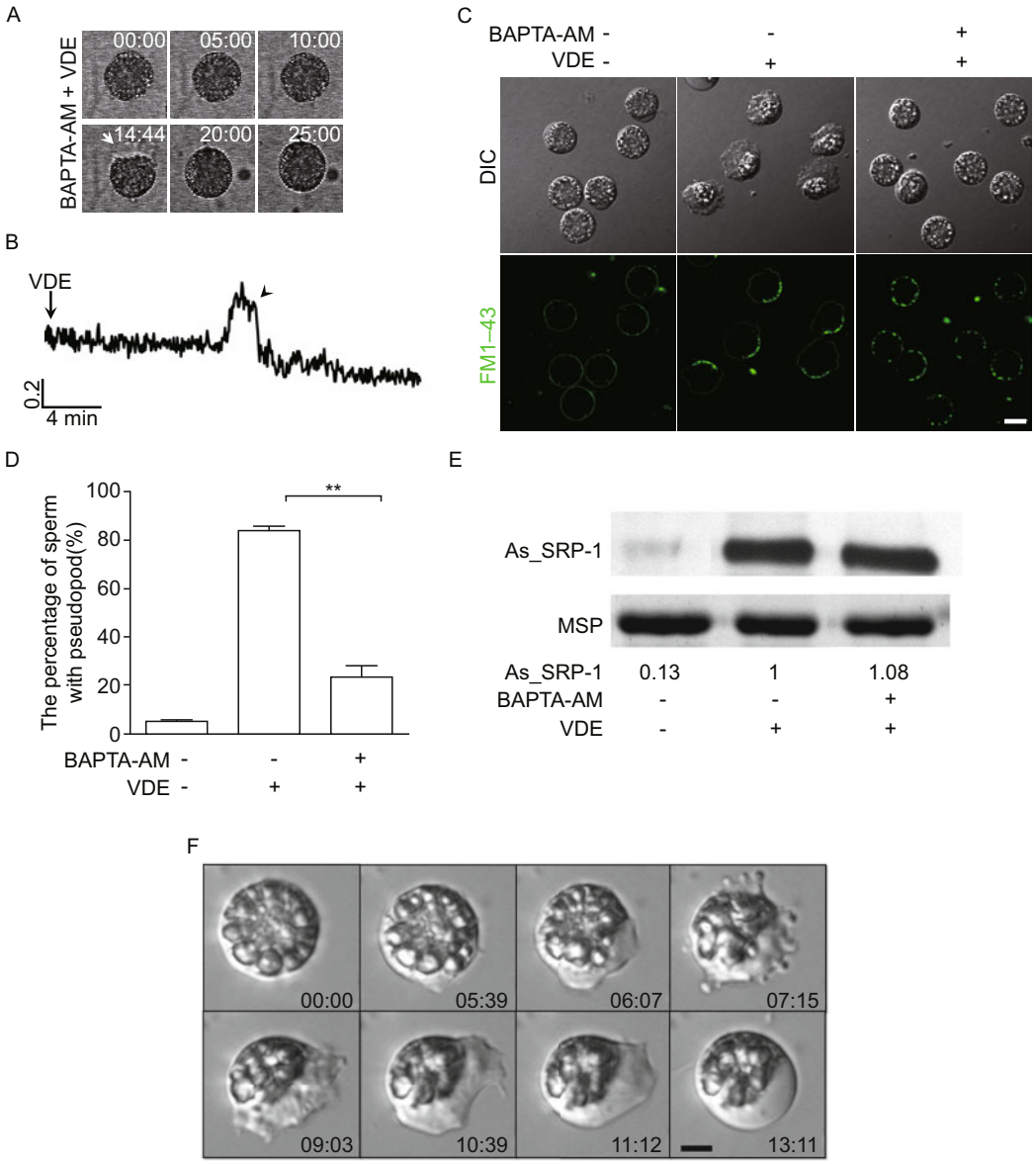

Figure 3. Depletion of cytosolic Ca^{2+} inhibits pseudopod extension by suppressing mitochondrial membrane potential. (A and B) The cell-permeable Ca^{2+}chelator, BAPTA-AM, blocks VDE-induced pseudopod formation (A) and the duration of Ca^{2+} oscillation (B). Spermatids were treated with 50 μmol/L BAPTA-AM, followed by treatment with VDE. The time-lapse images of morphological changes (A) and Fluo-4 fluorescence dynamics (B) were obtained simultaneously using confocal microscope. The arrow in (A) indicates a pseudopod and the arrowhead in (B) indicates one $[Ca^{2+}]_i$ oscillation. The abscissa axis: time (min); the vertical axis, ΔF/F0. Scale bar, 10 μm. (C) Pseudopod extension but not MO fusion was inhibited by BAPTA-AM. Sperm were treated with 50 μmol/L BAPTA-AM for 15 min and then stimulated with VDE for 10 min; sperm without treatment of BAPTA-AM served as controls. Scale bar, 10 μm. (D) Analysis of the inhibition of BAPTA-AM on pseudopod formation. Values are the mean ± SEM (n = 8). $^{**}P < 0.001$. (E) BAPTA-AM does not inhibit the secretion of As_SRP-1. Treatments were the same as in (C) but without FM1–43 staining. MSP served as the loading control. The As_SRP-1 bands were quantified and normalized and are shown below the immunoblot. (F) Artificially introducing Ca^{2+} back into sperm partially relieves the inhibitory effect of BAPTA-AM on pseudopod extension. Spermatids pretreated with BAPTA-AM were stimulated with VDE for 10 min, followed by being perfused with solutions containing BAPTA-AM, VDE, 2.5 μmol/L A23187 (Ca^{2+} ionophore) and 100 μmol/L Ca^{2+}. Timing was started as the perfusion was initiated. Scale bar, 5 μm.

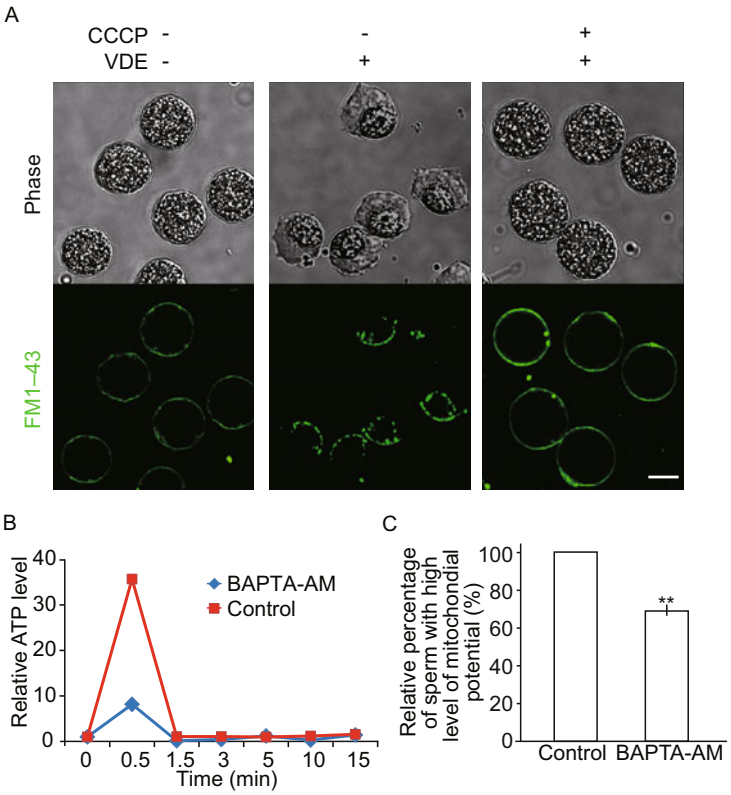

Figure 4. Ca^{2+} regulates sperm activation through mitochondria. (A) CCCP inhibits MO fusion and pseudopod extension. Upper panel shows Phase images of sperm treated with or without 10 μmol/L CCCP followed by VDE or H-VDE. Lower panel shows sperm stained with FM1–43 after the treatments. Scale bar, 10 μm. (B) Representative graph of intracellular ATP measurement after VDE stimulation in control and BAPTA-AM pretreated sperm. (C) Cytosolic Ca^{2+} depletion by BAPTA-AM decreases the mitochondrial potential. Spermatids treated with DMSO followed by VDE served as control for those treated with BAPTA-AM and VDE. The percentage of cells with a high level of mitochondrial membrane potential was normalized on the basis of controls. Values are the mean ± SEM (n = 12). $^{**}P < 0.001$.

blocking the Ca^{2+}-induced ATP production in mitochondria.

Calmodulin is involved in the regulation of pseudopod extension and MO fusion

As a Ca^{2+}-binding protein, calmodulin (CaM) mediates the interaction between Ca^{2+} and most of its targets (Krebs and Heizmann, 2007). Furthermore, CaM is involved in mammalian sperm capacitation and acrosome reaction (Si and Olds-Clarke, 2000; Bendahmane et al., 2001). Therefore, we explored whether Ca^{2+} regulates nematode sperm activation via CaM. Our FM1–43 staining assay revealed that the CaM inhibitors CPZ and TFP inhibited VDE-induced MO fusion (Fig. 5A). The As_SRP-1 secretion assay (Fig. 5C) and transmission electron microscopy (TEM) analysis of sperm structures (Fig. 5J and 5K; control cells are illustrated in Fig. 5D, 5E, 5G and 5H) also showed that CPZ or TFP inhibited VDE-triggered MO fusion. These facts suggest that CaM activity is required for MO fusion during sperm activation.

Interestingly, we found that pseudopod extension occurred in 48% and 46% of the TFP (150 μmol/L)- and CPZ (150 μmol/L)-treated spermatids, respectively. In contrast, only 5% of the H-VDE-treated control spermatids showed pseudopod protrusion (Fig. 5B). TEM analysis showed that MSP assembling was indeed initiated in the TFP-treated cells (Fig. 5I and 5L; controls are illustrated in Fig. 5F). This observation is in line with a previous study showing that the CaM inhibitor TFP, CPZ or W7 induced *C. elegans* sperm activation *in vitro* (Shakes and Ward, 1989).

Calcineurin inhibits assembly and promotes disassembly of MSP cytoskeleton

CaN, a Ca^{2+}/CaM-dependent serine/threonine phosphatase, has been identified in *C. elegans* sperm (Bandyopadhyay et al., 2002). Considering that protein phosphorylation/dephosphorylation regulates MSP dynamics (Italiano et al., 1996; Miao et al., 2003), we hypothesized that CaM inhibitor might induce pseudopod extension via decreasing the phosphatase activity of CaN. To test this hypothesis, we examined the effect of CaN on MSP assembly and disassembly. The assembly/disassembly status of MSP fiber can be indicated by increase/decrease of MSP fiber optical density (Roberts et al., 1998). We found that recombinant human CaN (25.6 nmol/L) not only significantly inhibited MSP assembly (Fig. 6A and 6B), but also promoted MSP filament disassembly *in vitro* (Fig. 6A and 6C). Consistently, increasing the CaN activity by introducing Ca^{2+} into the reconstitution system significantly inhibited the assembly and enhanced the disassembly of MSP fiber, simultaneously (Fig. 6D–F). Taken together, these results support the idea that Ca^{2+} plays dual roles in modulating MSP assembly. On the one hand, acting in a dominant pathway, Ca^{2+} promotes ATP production in the mitochondria, thereby enhancing MSP assembly. On the other hand, Ca^{2+} binds to CaM that then activates CaN, a phosphatase that inhibits assembly and promotes disassembly of MSP filament (Fig. 7).

DISCUSSION

Cell polarity is essential for the proper function of most differen-

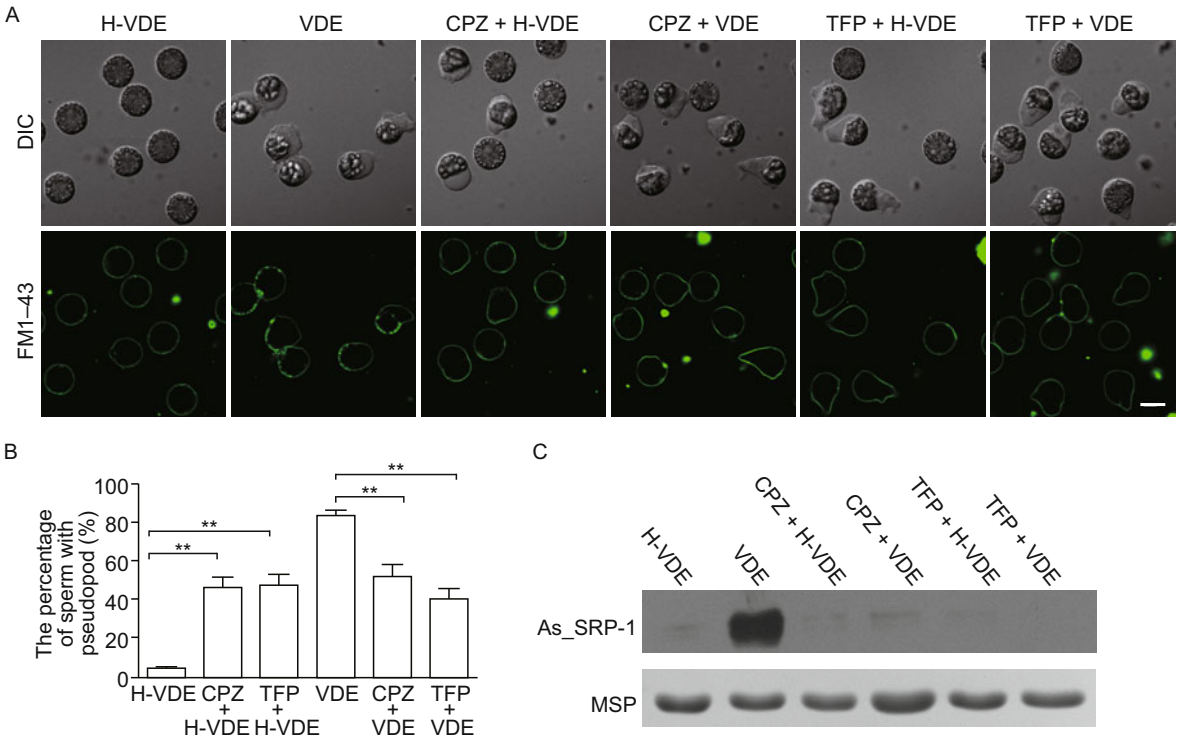

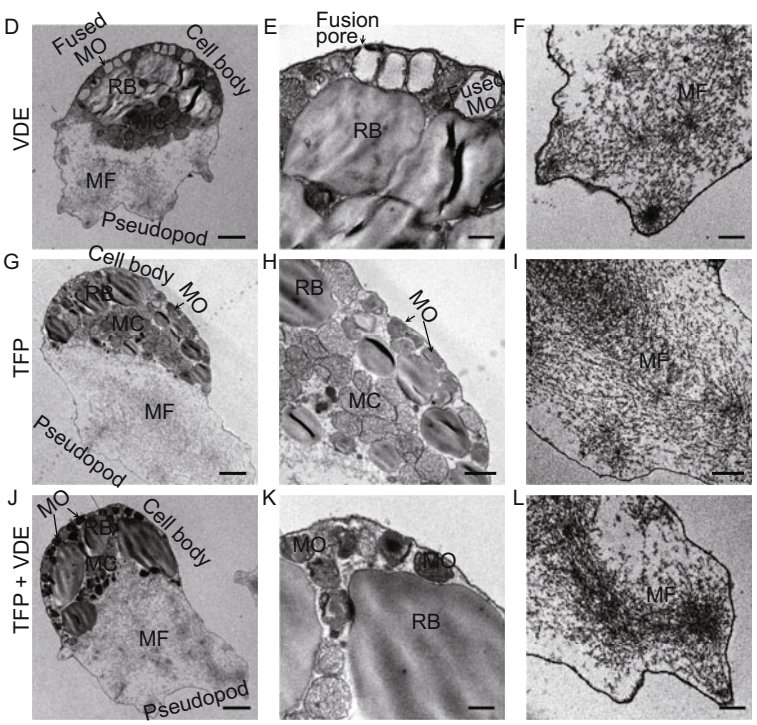

Figure 5. CaM inhibitors induce pseudopod extension and inhibit VDE-induced MO fusion. (A) Spermatids were pretreated with 150 μmol/L CPZ or TFP (CaM inhibitors) for 10 min and then stimulated with VDE or H-VDE. Sperm treated with VDE and H-VDE alone served as positive and negative controls, respectively. Scale bar, 10 μm. (B and C) The effects of CaM inhibitors on sperm pseudopod extension with statistics (B) and MO fusion using the As_SRP-1 secretion assay (C). Sperm were treated as in (A) but without FM1–43 staining. Values in (B) are the mean ± SEM (n = 23). $^{**}P < 0.001$. The MSP in (C) was used as a loading control. (D–L) TEM images show the effects of TFP on sperm pseudopod extension and MO-PM fusion. (D) Spermatids were activated with VDE. (E and F) High magnification images of sperm in (D). (G) Spermatids were treated with 150 μmol/L TFP. (H and I) High magnification images of sperm in (G). (J) Spermatids were treated with 150 μmol/L TFP, then with VDE. (K and L) High magnification images of cells in (J). MSP filaments (MFs), mitochondria (MC) and refringent bodies (RBs) are also shown in (D–L). Scale bars, 2 μm in D, G and J; 1 μm in H, I; 0.5 μm in E, F, K and L.

tiated cell types. Its establishment in response to extracellular stimuli is regulated spatially and temporally by complex regulatory pathways in migrating cells and is dependent on actin polymerization for pseudopodial extension. Sperm of nematodes lack the conventional actin machinery typically associated with amoeboid cell motility; instead, their activation and migration are dependent on the dynamics of the MSP-based cytoskeleton. Our study has shown that cytosolic Ca^{2+}, as a multifunctional modulator, is required for sperm activation in *Ascaris*. Thus, Ca^{2+} released from intracellular stores is required for increasing mitochondrial activity to provide sufficient energy required for sperm activation and migration. Because

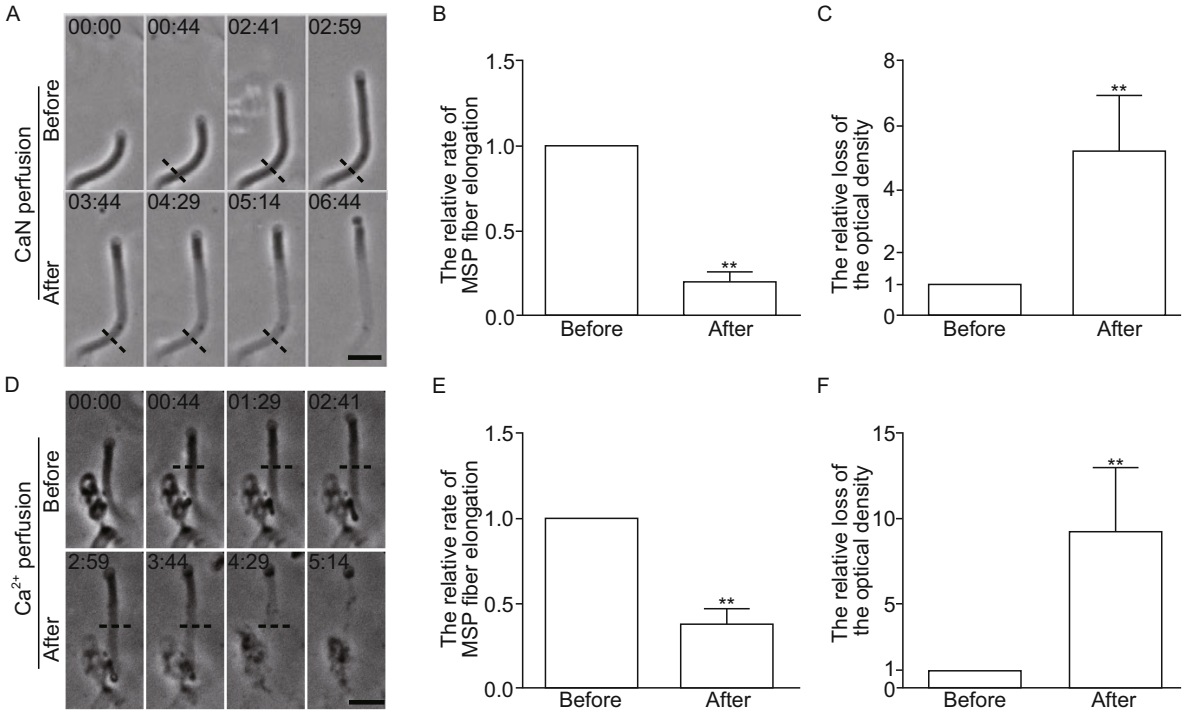

Figure 6. CaN inhibits MSP assembly and promotes MSP disassembly. (A) Normal MSP fiber was assembled in the *in vitro* reconstitution system containing 20% sperm extract and 200 μmol/L ATP and was perfused with new solution (containing 20% sperm extract, 200 μmol/L ATP and 25.6 nmol/L CaN). Time-lapse phase-contrast images of MSP fibers were captured with CCD camera. The dotted line indicates the site where optical density was measured. (B) The relative growth rate of MSP fibers in (A) before and after perfusion with CaN solution. Values are the mean ± SEM (n = 5). $^{**}P < 0.001$. (C) The relative loss of the optical density of MSP fibers at the dotted line during 2 min before and after starting perfusion. Values are the mean ± SEM (n = 5). $^{**}P < 0.05$. (D) The perfusion of additional 0.5 mmol/L Ca^{2+} significantly inhibits MSP fiber elongation and promotes MSP fiber disassembly. (E) The relative growth rate of MSP fibers in (D) before and after perfusion. Values are the mean ± SEM (n = 11). $^{**}P < 0.001$. (F) The relative loss of the optical density of MSP fibers at the dotted line during 2 min before and after starting perfusion with Ca^{2+} solution. Values are the mean ± SEM (n = 11). $^{**}P < 0.05$. All the time stamps are coded in format of min:sec. Scale bars, 5 μm in (A) and (D).

sperm are terminally differentiated cells and are quiescent transcriptionally and translationally, their maturation is highly dependent on post-translational modifications to the existing protein components. Protein phosphorylation and dephosphorylation of MSP cytoskeletal accessory proteins are necessary for modulating the assembly and disassembly of the MSP cytoskeleton at the leading and rear edges of the pseudopod, respectively (LeClaire et al., 2003; Miao et al., 2003; Yi et al., 2007; Yi et al., 2009). Phosphorylation sites in the MSP have also been identified in *C. elegans* (Fraire-Zamora et al., 2011). Thus, ATP appears to be used indirectly for pseudopod extension and Ca^{2+} plays a pivotal role in regulating sperm mitochondrial activity. On the other hand, Ca^{2+} negatively regulates the assembly and promotes the disassembly of MSP filaments by enhancing the activity of the CaN. The spatial and temporal regulation of cytoskeleton disassembly at the base of the pseudopod where it joins the cell body is necessary to generate the retraction force needed to pull the cell body forward (Shimabukuro et al., 2011). In addition, free disassembled MSP dimers are recycled to the leading edge, where they are reassembled to generate a protrusive force (Roberts, 2005; Miao et al., 2008). Ca^{2+} oscillations might provide a mechanism for local instead of global regulation of disassembling the MSP cytoskeleton.

Nematode spermatozoa are crawling cells, morphologically different from flagellated sperm. Exocytosis takes places at several sites over the cell body during nematode sperm activation, unlike the acrosome reaction that is a single vesicle fusion event in flagellated sperm. However, both types of sperm might share evolutionarily conserved components for vesicle fusion. In a variety of secretory cells, vesicle fusion is stimulated by an increase in $[Ca^{2+}]_i$, and this is detected by synaptotagmin, a C2 domain-containing protein located on the vesicle surface. We have shown here that both Ca^{2+} release from the intracellular store and the activity of CaM are required for fusion of the MO with the PM during sperm activation. Interestingly, CaM antagonists also block agonist-induced acrosome reaction in mouse sperm (Zeng and Tulsiani, 2003). Furthermore, the Ca^{2+}/CaM-dependent synaptotagmin VI is required for human sperm acrosomal exocytosis (Castillo Bennett et al., 2010).

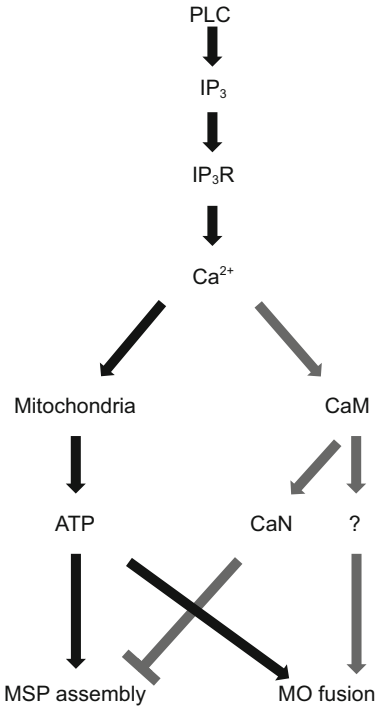

Figure 7. Proposed model of Ca^{2+} signaling transduction and function in *Ascaris suum* sperm activation. The sperm activator activates PLC through its receptor to generate IP_3, which triggers IP_3R to release Ca^{2+} from the intracellular Ca^{2+} store. The released Ca^{2+}, on the one hand, is taken up by mitochondria and increases mitochondrial membrane potential to boost ATP production; ATP may be further used in phosphorylation and other processes to promote MSP cytoskeleton assembly and MO fusion. On the other hand, after binding to CaM, Ca^{2+} regulates MO fusion via an unidentified factor and activates CaN to promote MSP disassembly. The coordination of Ca^{2+} release by IP_3R and recycling by Ca^{2+} pump generates $[Ca^{2+}]_i$ oscillations.

The existence and necessity of C2 domain-containing protein FER-1 for MO fusion in *C. elegans* indicates that nematode sperm, like human sperm (Blas et al., 2005), might utilize SNARE complex-mediated signaling cascades for the regulation of exocytosis.

MATERIALS AND METHODS

Sperm preparation and treatment

Ascaris suum male worms were collected from slaughterhouse and recovered in worm buffer (PBS buffer containing 10 mmol/L $NaHCO_3$, pH 7.0) at 38°C overnight. Spermatids were obtained by dissecting males, removing the seminal vesicle and extruding the seminal fluid into HKB buffer (50 mmol/L HEPES, 70 mmol/L KCl, 10 mmol/L $NaHCO_3$, pH 7.1). The isolated spermatids were stimulated to extend the pseudopods and mature into spermatozoa with the addition of VDE. To test the influences of various reagents on sperm activation, the spermatids were pretreated with reagents and activated by adding VDE. Live cells were pipetted into chambers formed by mounting a glass coverslip onto a glass slide with two parallel strips of double-sided tape and examined using a confocal microscope system (Olympus FV500 with a 60 × /1.4 NA oil immersion objective, Japan). For rescuing sperm from the inhibitory effects of a Ca^{2+} chelator, cells treated with BAPTA-AM (50 μmol/L) and VDE were perfused with a control solution (HKB containing 50 μmol/L BAPTA-AM, VDE and 2.5 μmol/L A23187) or a rescue solution (the control solution plus additional Ca^{2+}). Images were captured with a charge-coupled device (CCD; Andor Technology PLC, UK) coupled with an Axio Imager M2 microscope (Carl Zeiss, Germany) and processed with MetaMorph software (Universal Imaging, USA).

Examination of cytosolic Ca^{2+} dynamics

Spermatids were stained with 5 μmol/L Fluo 4-AM at 38°C for 15 min and then washed twice with HKB. The stained cells were then pipetted into a chamber fixed on the microscope stage and imaged at intervals of 4 s using the CCD camera coupled to Leica SP5 confocal microscopy system (Leica, Germany) at room temperature (λex 488 nm and λem 505 nm). During image collection, VDE or other reagents were applied gently into the chamber. The dynamics of fluorescence intensity which indicates the changes of $[Ca^{2+}]_i$ were analyzed using LAS AF software with the formula: ΔF/F0 = (F–F0)/F0 (ΔF/F0 represents the relative change of fluorescence intensity against the mean baseline fluorescence intensity F0).

FM1–43 staining and confocal microscopy

Spermatids were incubated in HKB buffer with or without VDE or other reagents and the treated cells were stained with FM1–43 (Molecular Probes, USA) at 5 μg/mL for 2 min to visualize fusion of the PM and MO upon activation (Washington and Ward, 2006). Images were captured using a confocal laser scanning microscope (Leica SP5 with a 40 × /1.25 NA oil-immersion objective, Germany).

As_SRP-1 secretion assay

This assay was performed as described in (Zhao et al., 2012). The amounts of As_SRP-1 secreted into the medium were shown by western blotting using an anti-As_SRP-1 antibody, while the loading control was indicated by the Coomassie Brilliant Blue staining of SDS-PAGE with cell samples.

Measurement of intracellular ATP concentration

The spermatids were treated with 50 μmol/L BAPTA-AM or BAPTA (control) for 15 min and then stimulated with VDE. The sperm at different time after VDE treatments were collected, lysed and centrifuged (12,000 r/min, 5 min, 4°C). The supernatant was subjected to ATP measurement using ATP Assay Kit (Beyotime, China).

Measurement of mitochondrial membrane potential

The spermatids were treated with 50 μmol/L BAPTA-AM or BAPTA (control) for 15 min and then stimulated with VDE. The sperm were stained for 20 min with JC-1 (5 μg/mL) (Beyotime, China) at 38°C and then rinsed twice with staining buffer. Finally, cells were analyzed using a flow cytometer (BD Biosciences, USA) with settings of λex 488 nm and λem 530 nm for monomers and λex 525 nm and λem 590 nm for

aggregates, and quantified the amounts of sperm with high and low mitochondrial potential.

Reconstitution of MSP filament assembly *in vitro*

MSP fiber reconstitution was performed as described (Shimabukuro et al., 2011). Sperm extract (20%) and ATP (0.2 mmol/L or 1 mmol/L) with or without other reagents were prepared in KPM buffer (10 mmol/L potassium phosphate, 0.5 mmol/L $MgCl_2$, pH 6.8) and pipetted into a chamber, and then examined on an Axio Imager A1 microscope (Carl Zeiss, Germany) equipped with a phase-contrast objective lens. The elongation rate and optical density of MSP filament were analyzed with MetaMorph software.

TEM of *Ascaris* sperm

Sperm were fixed with GTS-Fixative (2.5% glutaraldehyde, 2 mg/mL tannic acid and 0.5 mg/mL saponin in HKB) for 40 min on a Thermanox plastic coverslip (EMS, USA), followed by washing in HKB buffer and then water. They were post-fixed in 1% osmium tetroxide for 30 min, dehydrated in a graded series of ethanol followed by propylene oxide, and then infiltrated and embedded with EMbed-812 resin (EMS, USA). Ultrathin sections (80 nm) were cut on a Leica UC6 ultramicrotome, collected on formvar-coated copper grids and stained with uranyl acetate and lead citrate. TEM images were captured using an FEI Spirit 120 kV electron microscope (FEI Co., USA) operated at 100 kV.

ACKNOWLEDGMENTS

This work was supported by the National Basic Research Program (973 Program) (Nos. 2012CB945002 and 2010CB912303) and 31171337 from the Chinese government.

ABBREVIATIONS

CaM, calmodulin; CaN, calcineurin; H-VDE, heat-inactivated VDE; IP_3R, inositol (1,4,5)-trisphosphate receptor; MO, membranous organelle; MSP, major sperm protein; PLC, phospholipase C; PM, plasma membrane; TEM, transmission electron microscopy; VDE, vas deferens extract

COMPLIANCE WITH ETHICS GUIDELINES

Y.S. and L.M. designed the research; Y.S., L.C., Z.L. and X.W. performed the research; Y.S. and L.M. analyzed the data; and Y.S., X. M. and L.M. wrote the paper.

Yunlong Shang, Lianwan Chen, Zhiyu Liu, Xia Wang, Xuan Ma and Long Miao declare that they have no conflict of interest.

All institutional and national guidelines for the care and use of laboratory animals were followed.

REFERENCES

Abbas, M., and Foor, W.E. (1978). Ascaris suum: free amino acids and proteins in the pseudocoelom, seminal vesicle, and glandular vas deferens. Exp Parasitol 45, 263–273.

Bandyopadhyay, J., Lee, J., Lee, J.I., Yu, J.R., Jee, C., Cho, J.H., Jung, S., Lee, M.H., Zannoni, S., Singson, A., et al. (2002). Calcineurin, a calcium/calmodulin-dependent protein phosphatase, is involved in movement, fertility, egg laying, and growth in Caenorhabditis elegans. Mol Biol Cell 13, 3281–3293.

Ben-Aharon, I., Brown, P.R., Etkovitz, N., Eddy, E.M., and Shalgi, R. (2005). The expression of calpain 1 and calpain 2 in spermatogenic cells and spermatozoa of the mouse. Reproduction 129, 435–442.

Bendahmane, M., Lynch, C., 2nd, and Tulsiani, D.R. (2001). Calmodulin signals capacitation and triggers the agonist-induced acrosome reaction in mouse spermatozoa. Arch Biochem Biophys 390, 1–8.

Berridge, M.J. (2007). Calcium signalling, a spatiotemporal phenomenon. In New Comprehensive Biochemistry, K. Joachim, and M. Marek, eds. (Elsevier), pp. 485–502.

Berrios, J., Osses, N., Opazo, C., Arenas, G., Mercado, L., Benos, D.J., and Reyes, J.G. (1998). Intracellular Ca2+ homeostasis in rat round spermatids. Biol Cell 90, 391–398.

Blas, G.A.D., Roggero, C.M., Tomes, C.N., and Mayorga, L.S. (2005). Dynamics of SNARE assembly and disassembly during sperm acrosomal exocytosis. Plos Biol 3, e323.

Breitbart, H. (2002). Intracellular calcium regulation in sperm capacitation and acrosomal reaction. Mol Cell Endocrinol 187, 139–144.

Castillo Bennett, J., Roggero, C.M., Mancifesta, F.E., and Mayorga, L.S. (2010). Calcineurin-mediated dephosphorylation of synaptotagmin vi is necessary for acrosomal exocytosis. J Biol Chem 285, 26269–26278.

Estrada, M., Cárdenas, C., Liberona, J.L., Carrasco, M.A., Mignery, G.A., Allen, P.D., and Jaimovich, E. (2001). Calcium transients in 1B5 myotubes lacking ryanodine receptors are related to inositol trisphosphate receptors. J Biol Chem 276, 22868–22874.

Fraire-Zamora, J.J., Broitman-Maduro, G., Maduro, M., and Cardullo, R.A. (2011). Evidence for phosphorylation in the MSP cytoskeletal filaments of amoeboid spermatozoa. Int J Biochem Mol Biol 2, 263–273.

Griffiths, E.J., and Rutter, G.A. (2009). Mitochondrial calcium as a key regulator of mitochondrial ATP production in mammalian cells. Arch Biochem Biophys 1787, 1324–1333.

Gulbransen, B.D., Bashashati, M., Hirota, S.A., Gui, X., Roberts, J.A., MacDonald, J.A., Muruve, D.A., McKay, D.M., Beck, P.L., Mawe, G.M., et al. (2012). Activation of neuronal P2X7 receptor-pannexin-1 mediates death of enteric neurons during colitis. Nat Med 18, 600–604.

Italiano, J.E., Roberts, T.M., Stewart, M., and Fontana, C.A. (1996). Reconstitution in vitro of the motile apparatus from the amoeboid sperm of Ascaris shows that filament assembly and bundling move membranes. Cell 84, 105–114.

Kaupp, U.B., Kashikar, N.D., and Weyand, I. (2008). Mechanisms of sperm chemotaxis. Annu Rev Physiol 70, 93–117.

Kirichok, Y., Navarro, B., and Clapham, D.E. (2006). Whole-cell patch-clamp measurements of spermatozoa reveal an alkaline-activated Ca2+ channel. Nature 439, 737–740.

Krebs, J., and Heizmann, C.W. (2007). Calcium-binding proteins and the EF-hand principle. In New Comprehensive Biochemistry, K. Joachim, and M. Marek, eds. (Elsevier), pp. 51–93.

L'Hernault, S.W. (2009). The genetics and cell biology of spermatogenesis in the nematode C. elegans. Mol Cell Endocrinol 306, 59–65.

LeClaire, L.L., 3rd, Stewart, M., and Roberts, T.M. (2003). A 48 kDa integral membrane phosphoprotein orchestrates the cytoskeletal dynamics that generate amoeboid cell motility in Ascaris sperm. J Cell Sci 116, 2655–2663.

Li, R., and Gundersen, G.G. (2008). Beyond polymer polarity: how the

cytoskeleton builds a polarized cell. Nature reviews. Mol Cell Biol 9, 860–873.

Ma, X., Zhao, Y., Sun, W., Shimabukuro, K., and Miao, L. (2012). Transformation: how do nematode sperm become activated and crawl? Protein & Cell 3, 755–761.

Miao, L., Vanderlinde, O., Liu, J., Grant, R.P., Wouterse, A., Shimabukuro, K., Philipse, A., Stewart, M., and Roberts, T.M. (2008). The role of filament-packing dynamics in powering amoeboid cell motility. Proc Natl Acad Sci U S A 105, 5390–5395.

Miao, L., Vanderlinde, O., Stewart, M., and Roberts, T.M. (2003). Retraction in amoeboid cell motility powered by cytoskeletal dynamics. Science 302, 1405–1407.

Roberts, T.M. (2005). Major sperm protein. Curr Biol 15, R153–153.

Roberts, T.M., Salmon, E.D., and Stewart, M. (1998). Hydrostatic pressure shows that lamellipodial motility in Ascaris sperm requires membrane-associated major sperm protein filament nucleation and elongation. J Cell Biol 140, 367–375.

Roberts, T.M., and Stewart, M. (2000). Acting like actin. The dynamics of the nematode major sperm protein (msp) cytoskeleton indicate a push-pull mechanism for amoeboid cell motility. J Cell Biol 149, 7–12.

Shakes, D.C., and Ward, S. (1989). Initiation of spermiogenesis in C. elegans: A pharmacological and genetic analysis. Dev Biol 134, 189–200.

Shimabukuro, K., Noda, N., Stewart, M., and Roberts, T.M. (2011). Reconstitution of amoeboid motility in vitro identifies a motor-independent mechanism for cell body retraction. Curr Biol 21, 1727–1731.

Si, Y., and Olds-Clarke, P. (2000). Evidence for the involvement of calmodulin in mouse sperm capacitation. Biol Reprod 62, 1231–1239.

Smith, J.R., and Stanfield, G.M. (2011). TRY-5 is a sperm-activating protease in caenorhabditis elegans seminal fluid. PLoS Genet 7, e1002375.

Sperry, A.O. (2012). The dynamic cytoskeleton of the developing male germ cell. Biol Cell 104, 297–305.

Teves, M.E., Guidobaldi, H.A., Unates, D.R., Sanchez, R., Miska, W., Publicover, S.J., Morales Garcia, A.A., and Giojalas, L.C. (2009). Molecular mechanism for human sperm chemotaxis mediated by progesterone. PLoS One 4, e8211.

Ward, S., Hogan, E., and Nelson, G.A. (1983). The initiation of spermiogenesis in the nematode Caenorhabditis elegans. Dev Biol 98, 70–79.

Washington, N.L., and Ward, S. (2006). FER-1 regulates Ca2+ -mediated membrane fusion during C. elegans spermatogenesis. J Cell Sci 119, 2552–2562.

Yi, K., Buttery, S.M., Stewart, M., and Roberts, T.M. (2007). A Ser/Thr kinase required for membrane-associated assembly of the major sperm protein motility apparatus in the amoeboid sperm of Ascaris. Mol Biol Cell 18, 1816–1825.

Yi, K., Wang, X., Emmett, M.R., Marshall, A.G., Stewart, M., and Roberts, T.M. (2009). Dephosphorylation of major sperm protein (MSP) fiber protein 3 by protein phosphatase 2A during cell body retraction in the MSP-based amoeboid motility of Ascaris sperm. Mol Biol Cell 20, 3200–3208.

Zeng, H.T., and Tulsiani, D.R. (2003). Calmodulin antagonists differentially affect capacitation-associated protein tyrosine phosphorylation of mouse sperm components. J Cell Sci 116, 1981–1989.

Zhao, Y., Sun, W., Zhang, P., Chi, H., Zhang, M.J., Song, C.Q., Ma, X., Shang, Y., Wang, B., Hu, Y., et al. (2012). Nematode sperm maturation triggered by protease involves sperm-secreted serine protease inhibitor (Serpin). Proc Natl Acad Sci U S A 109, 1542–1547.